Supplementary Information (SI) for Nanoscale.
This journal is © The Royal Society of Chemistry 2024

Supporting Information for

Amino-Functionalization Enhanced CO_2 Reduction Reaction in Pure Water

Junfeng Chen, [a] Wenzhe Niu, [a] Liangyao Xue, [a] Kai Sun, [a] Xiao Yang, [a] Xinyue Zhang, [a] Weihang Li, [a] Shuanglong Huang, [a] Wenjuan Shi, *[a] Bo Zhang, *[a]

[a]State Key Laboratory of Molecular Engineering of Polymers, Department of Macromolecular Science, Fudan University, Shanghai 200438, China.

*Corresponding author:

Methods

Materials

The ultrapure water (18.2 MΩ·cm^{-1}) used in all experiments was prepared by passing through an ultra-pure purification system. Silver nitrate (≥99.8%), methanol (≥99.5%), ethanol (≥99.7%), isopropanol (≥99.7%), potassium bicarbonate (≥99.5%), potassium hydroxide (≥85.0%), melamine (≥99.0%), dimethylformamide (≥99.5%), acetone (≥99.0%), ammonia water (25~28%), hydrochloric acid (36.0~38.0%), sodium nitrite(≥99.5%) were purchased from Sinopharm Chemical Reagent Company. Amorphous carbon powders (Vulcan XC72) were purchased from Suzhou Sinero Technology company. The Nafion solution (Dupont, D-520 dispersion, 5 wt% in water and 1-propanol) was purchased from Alfa Aesar. Sigracet 39BC GDL, the Sustainion solution (XA-9) and an anion exchange membrane (Sustainion X37-50 Grade RT) were purchased from Fuel Cell Store. All chemicals, including precursors, solvents, hydrophobic agents and ionomers, unless otherwise stated, were used without further purification.

Preparation of the amino-modified carbon powder:

Melamine (504 mg) was dissolved in 200 mL of deionized water. This solution was then added to carbon Vulcan XC72 (500 mg) and the mixture was stirred until an emulsion was formed. Then, sodium nitrite (287 mg) was added followed by the addition of concentrated HCl (5 ml). The mixture was stirred for 12 h and thereafter filtered over a nylon membrane having a pore size of 0.45 μm. The powder was then washed with successive aliquots of water, DMF, methanol and acetone. Finally, the amino-modified carbon powder was dried in a vacuum oven at 60 ℃ for 6 hours, yielding a high-purity product. When preparing carbon powder with different amino-modified content, the quantities of melamine, water, sodium nitrite and hydrochloric acid are increased proportionally. The preparation of the amino-modified carbon powder had been optimized.

Preparation of silver-based catalyst:

Silver nitrate (170 mg) was dissolved in water (10 mL), followed by the slow addition of concentrated ammonia water (250 μL), with vigorous shaking to obtain a clear silver-ammonia solution. Carbon powder (200 mg) was then dispersed in a mixed solution of water (50 mL) and ethanol (50 mL), to which the silver-ammonia solution (3 mL) was added. Subsequently, concentrated ammonia water (1.2 mL) was added slowly. The mixture was placed in a water bath at 50 °C for 14 h and thereafter filtered over a nylon membrane having a pore size of 0.45 μm. The powder was then washed with successive aliquots of water and ethanol, each thrice. Finally, the silver-based catalyst was dried in a vacuum oven at 60 ℃ for 6 hours, yielding a high-purity product. The Ag nanoparticle ‘s deposition had been optimized.

Preparation of gas diffusion electrodes (GDEs).

In the fabrication of Gas Diffusion Electrodes (GDE), a catalyst ink was prepared by

homogeneously mixing 12 mg of catalysts with methanol (2.7 mL), water (0.3 mL) and Nafion solution (60 μL), followed by sonication to ensure uniform dispersion. This slurry was then carefully applied onto a 2 cm × 2 cm Gas Diffusion Layer (GDL) using a drip-coating technique. Subsequently, a mixture of Sustainion (100 μL) solution and ethanol (1 mL) was sprayed onto the GDE. The conversion to hydroxide form is then achieved by treatment with a 1 M KOH solution.

Structural characterization.

Scanning Electron Microscopy (SEM) analysis was conducted on a Hitachi FE-SEM S-4800, operated at an accelerating voltage of 1.0 kV, providing detailed surface morphology insights. High-Resolution Transmission Electron Microscopy (HRTEM) images were captured using a JEOL JEM-2100F transmission electron microscope, functioning at 200 kV. Scanning Transmission Electron Microscopy (STEM) investigations were performed on two sophisticated instruments: an FEI Titan Cubed 60-300, operating at a high accelerating voltage of 300 kV and a JEOL ARM-200F equipped with a cold field emission gun and a CEOS-corrected Cs probe, at an operating voltage of 200 kV. X-ray Photoelectron Spectroscopy (XPS) was carried out on a PHI 5700 ESCA System, employing Al Kα X-ray radiation (1486.6 eV) for excitation. Powder X-ray Diffraction (XRD) patterns were acquired using a MiniFlex600 instrument, operating in Bragg-Brentano mode. The instrument was configured with a 0.02 ° divergence and a scan rate of 0.1 $°s^{-1}$. The adsorption-desorption isotherms of CO_2 were obtained using Micromeritics ASAP 2460 at conditions of 298 K and 1 atm. The Fourier Transform Infrared Spectrometer (FTIR) measurements were conducted using a Bruker INVENIO S, employing the KBr pellet method for sample preparation. Zeta potential measurements were conducted with a Malvern Instruments ZS90 apparatus, the test samples were catalyst suspensions at a concentration of 0.05 $mg·mL^{-1}$, dispersed in ultrapure water (18.2 $MΩ·cm^{-1}$). If not specified, the sample tested before the electrochemical activity is a powder sample. The samples tested after the reaction are electrodes.

Temperature programmed desorption (TPD).

For the CO_2 adsorption studies, a sophisticated TPD apparatus equipped with a thermal conductive detector (AutoChem II 2920) was employed. The catalysts underwent a degassing process at 100°C under a continuous flow of Helium (He) gas, effectively removing any pre-adsorbed gases from the catalyst surface. This process lasted for 1 hour, ensuring thorough preparation of the catalysts for subsequent CO_2 adsorption. Following degassing, CO_2 gas was introduced to the system, allowing for ample adsorption onto the catalysts. Excess CO_2 was then purged using Helium. The TPD sequence was initiated under a steady He flow at a constant velocity, facilitating the transport of desorbed CO_2 molecules to the detector. This methodology provided a detailed understanding of CO_2 adsorption and desorption dynamics on the catalyst surfaces, crucial for elucidating their catalytic behavior and efficiency in electrochemical processes.

Operando attenuated total reflection surface-enhanced infrared absorption spectroscopy (ATR-SEIRAS):

Firstly, the Au film was deposited on the reflecting plane of the Si prism according to the 'two-step wet process'. Different Ag-based catalysts coated on the Au/Si substrate were used as the working electrode. A Hg/HgO electrode and a graphite rod were applied as the reference and counter electrodes, respectively. The electrolyte was 0.5 M KHCO3 with CO_2 during the experiment. The electrode potential was altered from −0.41 V to −1.91 V versus the reversible hydrogen electrode (RHE) in a stepwise manner. Concurrently, the infrared spectra were recorded with a time resolution of 30 s per spectrum at a spectral resolution of 4 cm^{-1}.

The electrode potentials were rescaled to the RHE reference using the following equation:

$$E_{(vs.\ RHE)} = E_{(vs.\ Hg/HgO)} + 0.098\,V + 0.0591\,pH$$

Electrochemical measurements.

The zero-gap CO_2 electrolyzer was assembled from two specially customized titanium plates, incorporating a reaction area of 1 cm^2. The anode electrode was composed of IrO_2/Ti, with the catalyst uniformly sprayed onto treated titanium felt at a density of 3 $mg \cdot cm^2$. An anionic ion-exchange membrane, Sustainion X37-50 Grade RT was used, after pre-soaking in 1M KOH for 48 h During assembly, polytetrafluoroethylene (PTFE) spacers of specific thickness were used to separate the two electrode plates, arranged in the order of cathode plate-cathode electrode-ion exchange membrane-anode electrode-anode plate for tight assembly. In the testing process: on the anode side, a peristaltic pump was used to uniformly introduce ultrapure water at a constant temperature of 50 °C. On the cathode side, an Alicat Scientific mass flow controller was employed to maintain a CO_2 flow rate of 20 sccm, with the product gases directed into a gas chromatograph for analysis. The actual flow rate within the system was accurately determined using a bubble flowmeter located at the outlet of the cathodic chamber. This comprehensive setup ensured precise control over the experimental conditions, vital for the reliable assessment of CO_2RR catalytic performance. A Kikusui constant current source provided the electrical energy and recorded the full cell voltage and current during the reaction process.

Electrochemical impedance spectroscopy(EIS)

The EIS of various catalysts was measured in a homemade flow-cell configuration consisting of a gas chamber, a cathodic chamber, and an anodic chamber. The as-prepared working electrode was fixed between the gas and cathodic chambers, with the catalyst layer side facing the cathodic chamber (geometric active surface area of 1 cm^2). The Ni foam electrode and the Hg/HgO electrode (with 1 M KOH as the filling solution) were employed as counter and reference electrodes. The AEM was used to separate the cathode and the anode chambers.

The electrode potentials were rescaled to the RHE reference by the following equation:

$$E_{(vs.\,RHE)} = E_{(vs.\,Hg/HgO)} + 0.098\,V + 0.0591\,pH$$

The combined catalyst and diffusion layer, AEM and nickel anode were then

positioned and clamped together using polytetrafluoroethylene (PTFE) spacers such that 0.5 M $KHCO_3$ electrolytes could be introduced into the chambers between the anode and membrane, as well as the membrane and the cathode, at 10 mL·min^{-1} using a peristaltic pump. The supplied CO_2 (Air France, 99.9%) flow was kept constant at 20 mL·min^{-1} using an Alicat Scientific mass flow controller. The actual flow rate was determined using a bubble flowmeter at the outlet of the cathodic chamber.

Product analysis

The gas products (CO, H_2) were analyzed online continuously using a gas chromatograph (Ruimin Technologies, GC2060). The gas chromatograph was equipped with a packed TDX-01 column, a packed 5A column and Porapak T column. Argon (Shanghai TOMOE gases, 99.999%) was used as the carrier gas. Gas chromatography was calibrated using certified standard gases in advance and the FE of the products was calculated as follows:

$$FE = \frac{\varphi V P n F}{j \quad RT} \times 100\%$$

where φ is the volume fraction of CO or H_2, V represents the CO_2 gas flow rate, and j is the total current from the potentiostat. P, n, F, R *and* T are pressure, number of electrons transferred, Faraday's constant, ideal gas constant and temperature, respectively.

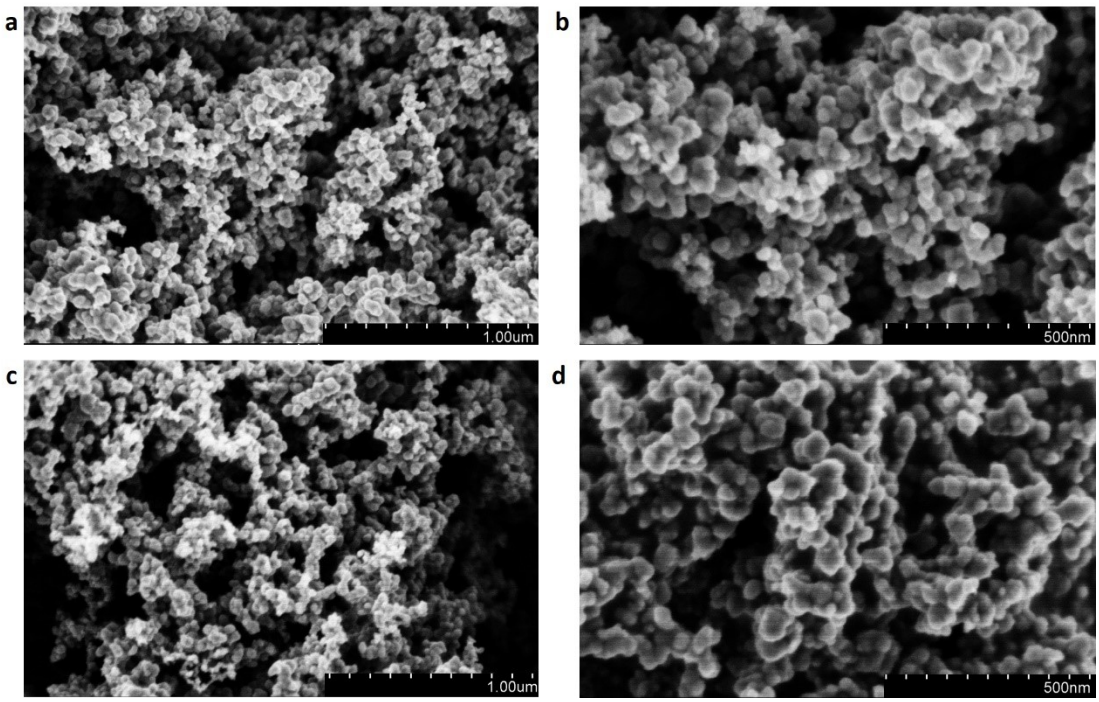

Figure S1. SEM images of the different samples. SEM images of (a-b) the Ag-C, (c-d) the Ag-C-Mel. Scale bar, 1 μm and 500 nm, respectively.

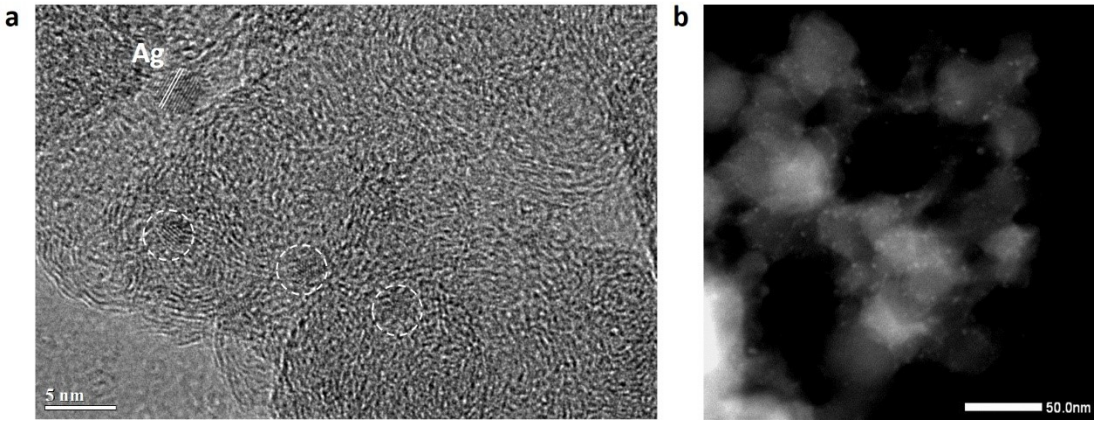

Figure S2. TEM images of the Ag-C samples. (a) HRTEM images of the Ag-C samples. Scale bar, 5 nm. (b) STEM images of the Ag-C. Scale bar, 50 nm.

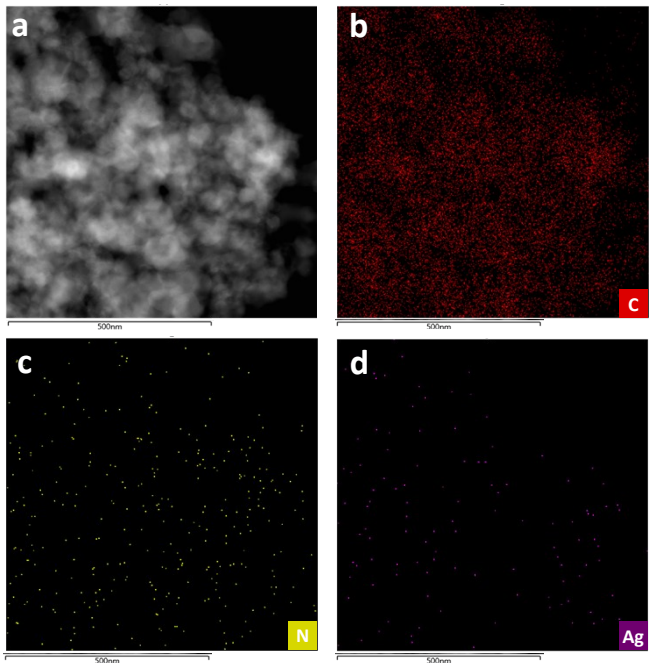

Figure S3. Energy-dispersive X-ray spectroscopy (EDS) elemental mapping images of Ag-C-Mel.

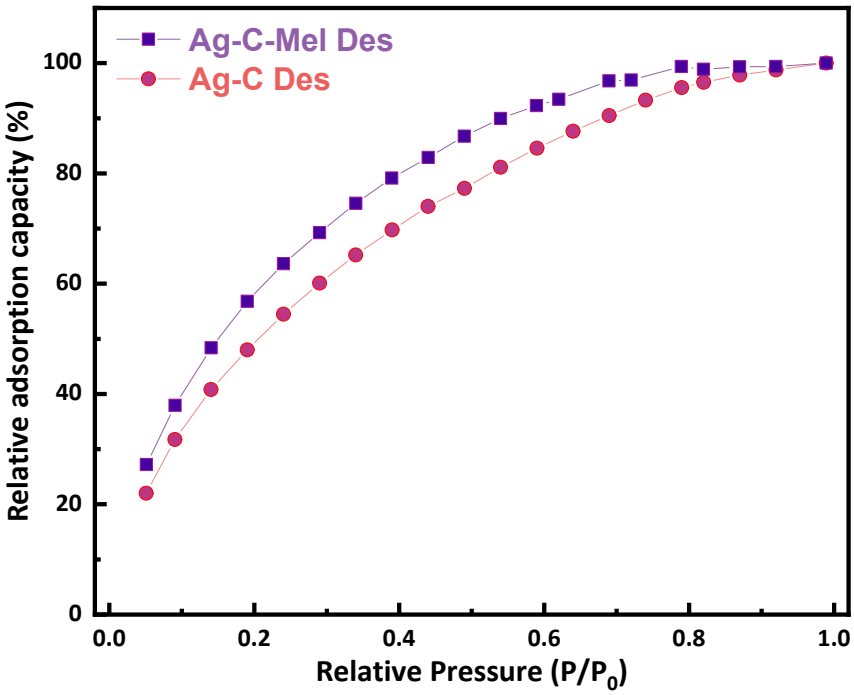

Figure S4. The CO_2 adsorption capacity of different catalysts relative to their maximum adsorption capacity during the CO_2 desorption process.

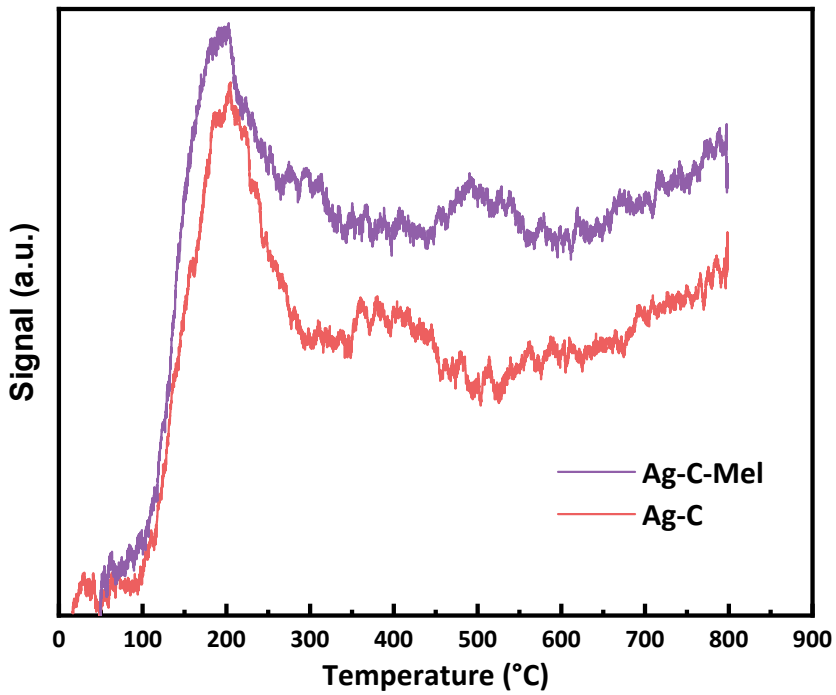

174

175 **Figure S5.** CO_2-TPD of the Ag-C-Mel and the Ag-C catalysts.

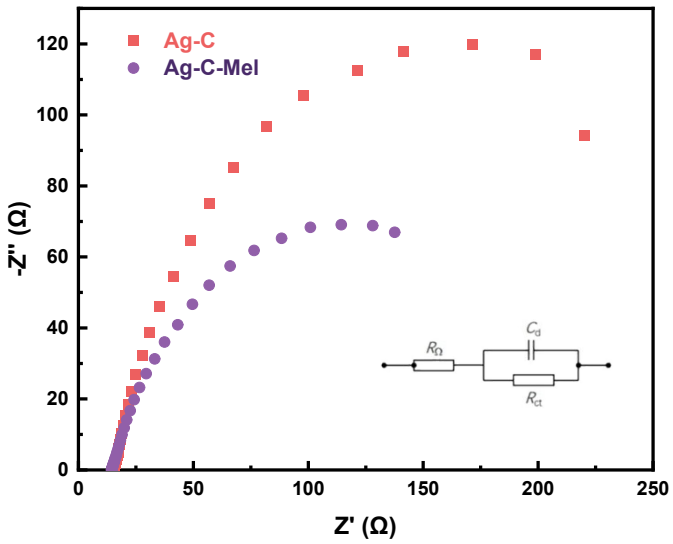

176

177 **Figure S6.** EIS Nyquist plots and equivalent circuit (inset) at −0.5 V vs. RHE.

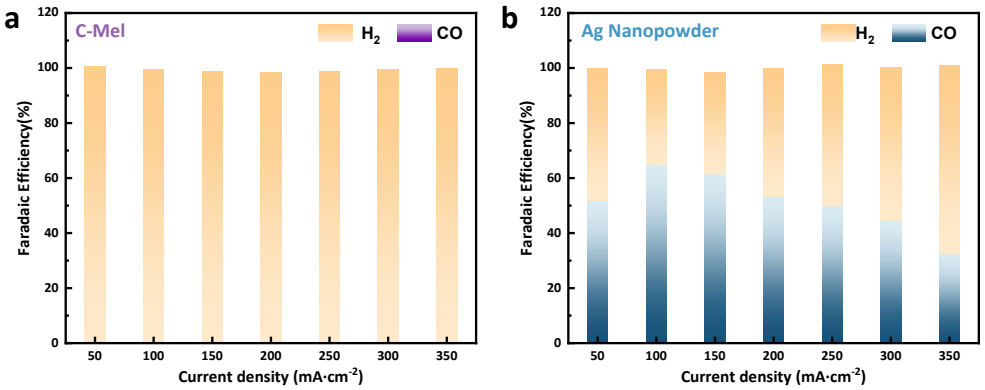

Figure S7. The CO_2RR performance of the C-Mel and the Ag nanopowder in zero-gap CO_2 electrolyzer utilizing pure water. (a, b) CO_2RR products distribution under different current densities for (a) the C-Mel and (b) the Ag nanopowder.

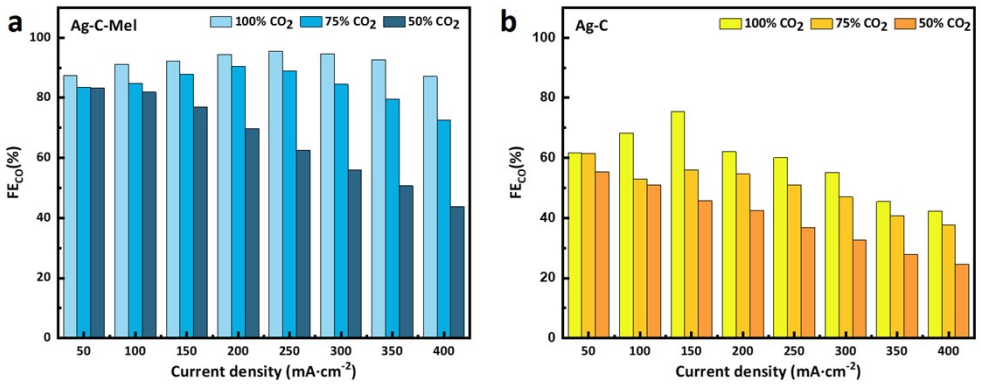

Figure S8. The FE_{CO} of (a) the Ag-C-Mel and (b) the Ag-C catalysts at different CO_2 partial pressures.

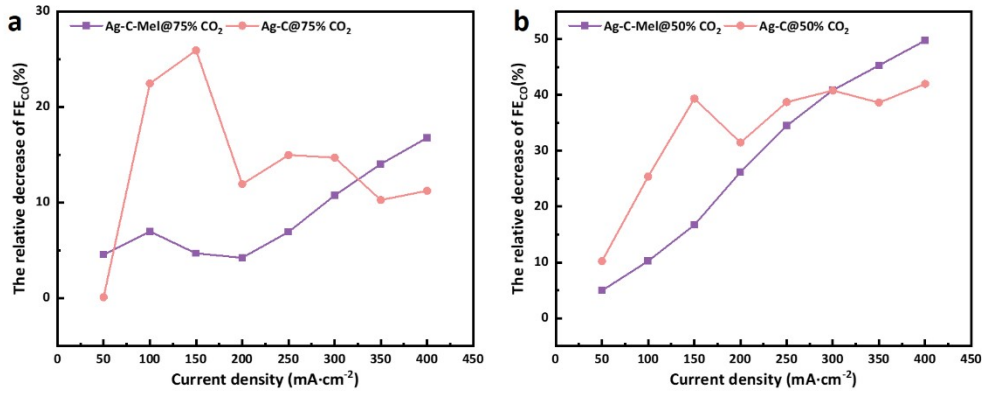

185

186 **Figure S9.** The relative decrease of FE_{CO} of the Ag-C-Mel and the Ag-C catalysts
187 under different CO_2 partial pressure compared with FE_{CO} under 100% CO_2 partial
188 pressure, (a) 75% CO_2 partial pressure, (b) 50% CO_2 partial pressure.

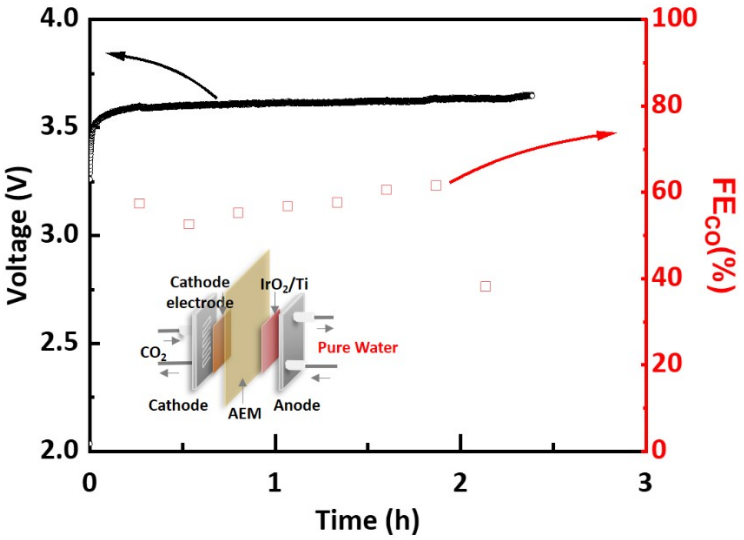

Figure S10. Continuous measurement of the Ag-C at the current density of 250 mA·cm^{-2}.

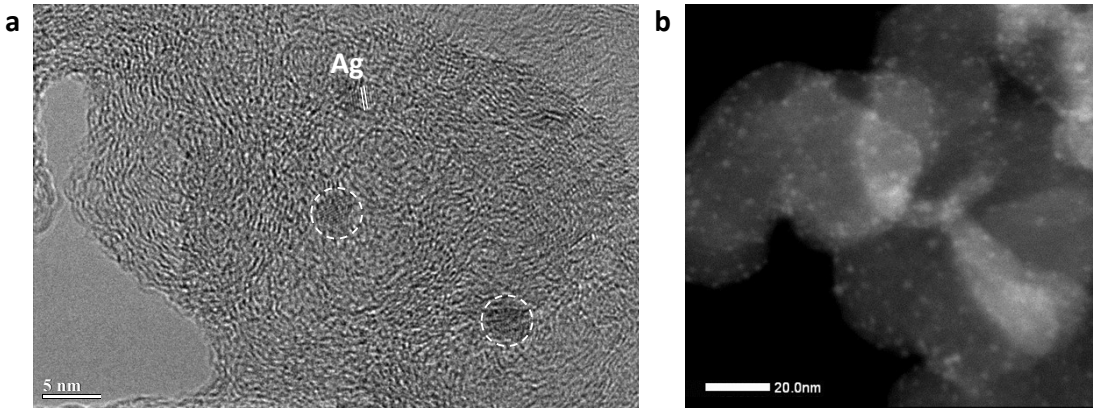

Figure S11. TEM images of the Ag-C-Mel samples after electrochemical activity. (a) HRTEM images of the Ag-C-Mel samples after electrochemical activity. Scale bar, 5 nm. (b) STEM images of the Ag-C-Mel samples after electrochemical activity. Scale bar, 50 nm.

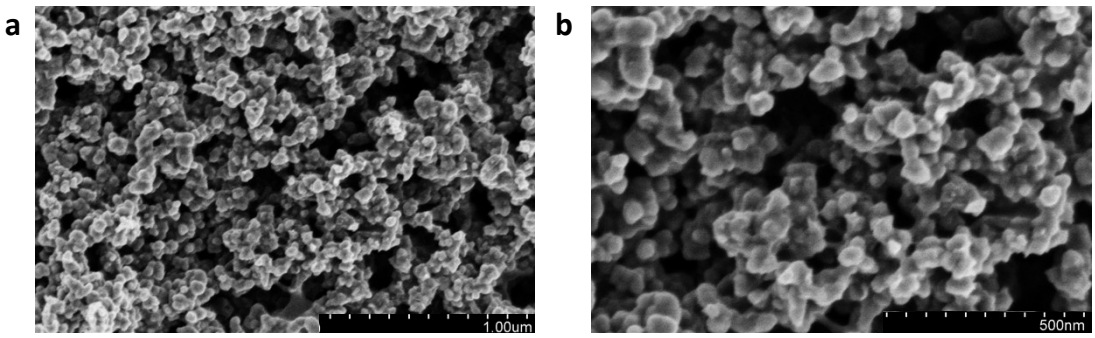

Figure S12. SEM images of the Ag-C-Mel after electrochemical activity. Scale bar, 1 μm and 500 nm, respectively.

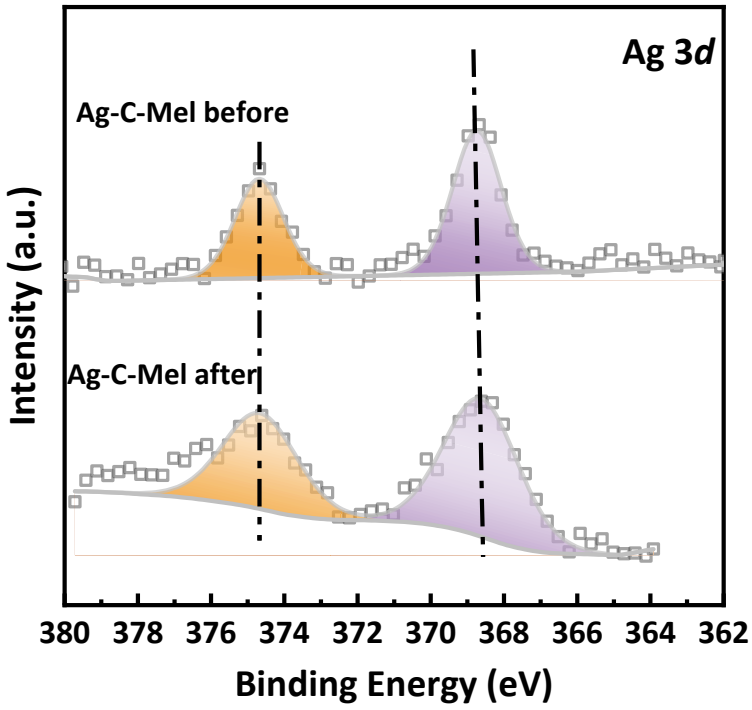

200

201 **Figure S13.** Ag 3*d* spectra of the Ag-C-Mel before and after electrochemical activity.

202 **Table S1 ICP results of different samples.**

Sample	Element	Mass content(%)
Ag-C	Ag	3.286
Ag-C-Mel	Ag	2.256

203